International Journal Of Renewable Energy Research, IJRER
S.Belfedhal, E.Berkouk, Vol.1, No3, pp.43-52 ,2011

Modeling and Control of Wind Power Conversion System with a Flywheel Energy Storage System

Seifeddine Belfedhal*, El-Madjid Berkouk**

*University of Ibn Khaldoun Tiaret, Algeria
**Laboratery of control process, ENP, Algiers, Algeria

e-mail: seifeddinebelfedhal@yahoo.fr, emberkouk@yahoo.fr

Received : 17.05.2011 Accepted : 18.06.2011

Abstract: In this paper, a control of a variable speed wind generator (VSWG) system based on a doubly fed induction machine connected to the network associated to a flywheel energy storage system (FESS) is considered. The maximum power point tracking (MPPT) method, the independent control power of generator, the grid connection, and the control of flywheel energy storage system are studied. The flywheel energy storage system consists of a power electronic converter supplying a squirrel-cage induction machine coupled to a flywheel. In order to validate the control method, the model of the system is simulated for different wind generator operating modes.

Keywords: MPPT, Doubly fed induction generator, Variable speed wind turbine, Independent power control, Flywheel energy storage system.

1. Introduction

The use of wind energy has indeed been growing: In late 2001, over 24 GW of wind power capacity was installed worldwide with an increase of 6 GW only in this year. It provides, in the world, the installation of wind farms with a capacity of 45,000 MW. They must provide up to 1000 MW per unit [1]. Variable speed wind turbines have been widely used because of their benefits. We can mention:

the decrease of the stresses on the mechanical structure, acoustic noise reduction, the possibility of active and reactive power control, and possibility of maximum power extraction by speed adaptation. A new large wind power has been developed based all on variable speed wind turbine using a direct-driven synchronous generator (without gearbox) or a doubly fed induction generator which is considered particularly in this study.

The main advantage of the DFIG is that the power electronics equipment only carries a fraction of the total power (20-30%) [2]. This means that the losses in the power electronics converters, as well as the costs, are reduced. Among the drawback of wind energy is that is very fluctuant because of the random and intermittent wind nature. Despite that, the development of this type of production is remarkable [1].

Several studies [3, 4, 5, 6, 7] have been concentrated around the regulation of power produced to ensure the balance between production and consumption by exploiting the idea of storing energy that the operating principle is to store excess power under kinetic energy form in the flywheel. The energy stored will be reconverted into the electrical form for use as a top up in case of deficit. FESS may thus be used as power regulators over short periods of time for electrical power quality improvement.

In order to analyze the behavior of VSWG associated to the FESS, the model of this global system is developed and simulated(Fig.1).

The wind turbine, gearbox, DFIG, AC-DC-AC converter, grid connection and FESS are modeled.

The maximum power point tracking (MPPT) algorithm to maximize the generated power is presented.

In order to study the power transfer between the wind generator and the network, we applied a control independent power. The storage system considered in this study consists of an electronic converter; an induction machine which operates in flux weakening region and a flywheel. The field oriented control will be considered here for the induction machine.

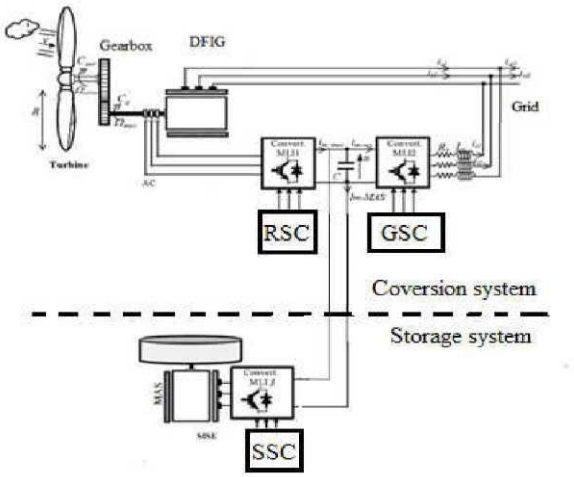

Fig. 1 Wind energy conversion and storage system (WECSS).

2. Wind conversion system

2.1 Wind turbine model

The turbine is characterized by its power coefficient Cp which is function of the tip speed ration and the pitch angle of specific wind turbine blades. For the used turbine, this coefficient is given by the following mathematical approximation:

$$C_p = 0.5 - 0.167.(\beta - 2).\sin\left[\frac{\pi.(\lambda + 0.1)}{18.5 - 0.3.(\beta - 2)}\right] - 0.00184.(\lambda - 3).(\beta - 2) \quad (1)$$

This relationship is shown on fig.2.

This graph is a key element in the characterization of wind energy converters [8, 10].

The tip speed ration is dependent on the wind speed and the turbine angular velocity:

$$\lambda = \frac{\Omega_{turbine}.R}{\upsilon} \quad (2)$$

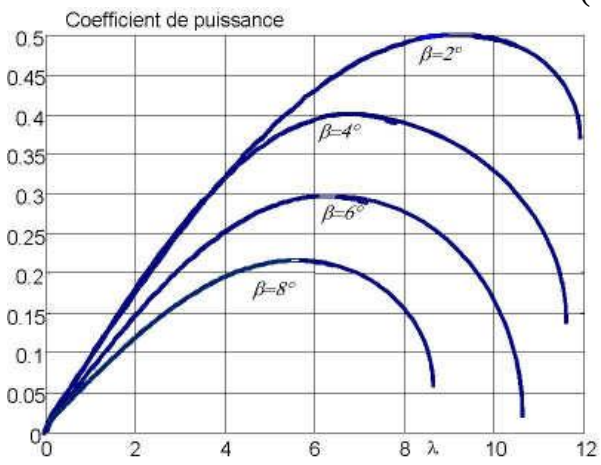

Fig. 2. Power coefficient [9]

A power available on the shaft of the turbine is given by:

$$P_{aer} = C_p(\lambda, \beta).\frac{\rho.S.\upsilon^3}{2} \quad (3)$$

The turbine torque is given by:

$$C_{aer} = \frac{P_{aer}}{\Omega_{turbine}} = C_p.\frac{\rho.S.\upsilon^3}{2}.\frac{1}{\Omega_{turbine}} \quad (4)$$

The gearbox is modeled by these two equations:

$$C_g = \frac{C_{aer}}{G} \quad (5)$$

$$\Omega_{turbine} = \frac{\Omega_{mec}}{G} \quad (6)$$

It is clear that the power extracted from the wind is maximized when Cp is maximized. This optimal value of Cp occurs at a defined value of the tip speed ratio _. For each wind speed, there is an optimum rotor speed where maximum power is extracted from the wind. Therefore, if wind speed is assumed to be constant, the value of Cp depends only on the rotor speed of the wind turbine. Thus, controlling the rotor speed controls the power output of the turbine. The variability of the output power from the wind generator implies that, without special interface measures, the turbine will often operate away from its maximum power

point. The associated losses can be avoided by the use of maximum power point tracker (MPPT) which ensures that there is always maximum energy transfer from the wind turbine to the grid. In this paper we develop the MPPT algorithm named "Perturbation and Observation Method". It is more accurate since it doesn't need the turbine characteristic measurement, and it is easier to implement [4, 5, 14].

This algorithm can be summarized as follow:

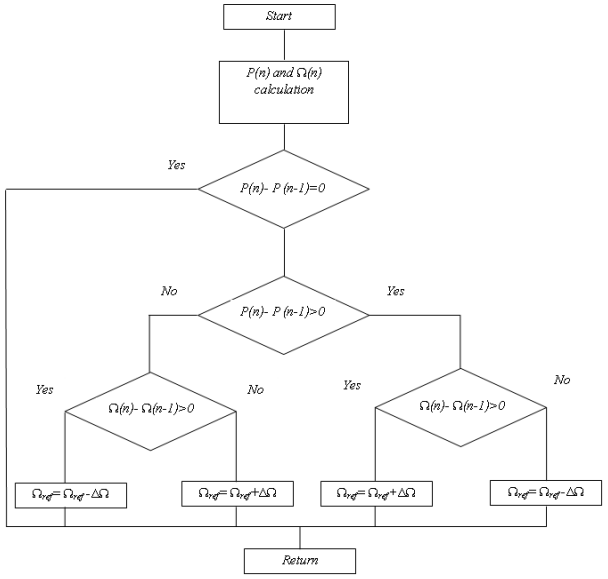

Fig.. 3. Flowchart of perturbation and observation method for maximum power point tracking.

2.2 DFIG model

The electrical equations in the PARK reference frame are given by:

$$\begin{cases} V_{ds} = R_s I_{dr} + \dfrac{d}{dt}\psi_{ds} - \omega_s \psi_{qs} \\ V_{qs} = R_s I_{qs} + \dfrac{d}{dt}\psi_{qs} + \omega_s \psi_{ds} \end{cases} \quad (7)$$

$$\begin{cases} V_{dr} = R_r I_{dr} + \dfrac{d}{dt}\psi_{dr} - (\omega_s - \omega)\psi_{qr} \\ V_{qr} = R_r I_{qr} + \dfrac{d}{dt}\psi_{qr} + (\omega_s - \omega)\psi_{dr} \end{cases} \quad (8)$$

The stator and rotor flux are written as follows:

$$\begin{cases} \psi_{ds} = L_s I_{ds} + M_{sr} I_{dr} \\ \psi_{qs} = L_s I_{qs} + M_{sr} I_{qr} \end{cases} \quad (9)$$

$$\begin{cases} \psi_{dr} = L_r I_{dr} + M_{sr} I_{ds} \\ \psi_{qr} = L_r I_{qr} + M_{sr} I_{qs} \end{cases} \quad (10)$$

The electromagnetic torque is defined as:

$$C_{em} = P\left(\psi_{ds} I_{qs} - \psi_{qs} I_{ds}\right) \quad (11)$$

The stator active and reactive powers at the stator are defined as:

$$\begin{cases} P_s = V_{ds} I_{ds} + V_{qs} I_{qs} \\ Q_s = V_{qs} I_{ds} - V_{ds} I_{qs} \end{cases} \quad (12)$$

PWM are employed for the all respective converters of the system (three converters) in order to produce a controlled output voltage vector [1, 14,17].

3. Conversion system control

3.1 Rotor side converter control

The control of rotor side converter is based on an active and reactive DFIG power control. So it controls independently the active and reactive powers generated by the DFIG by controlling independently the rotor currents of the DFIG (Fig. 4). Rotor current vector components are controlled by controlling the inverter voltage vector A d–q reference frame synchronized with the stator flux is employed [12]. By setting the quadratic component of the stator flux to the null value as follows:

$$\{\psi_{ds} = \psi_s \ , \ \psi_{qs} = 0 \quad (13)$$

Simplified expression of the electromagnetic torque is obtained:

$$C_{em} = -p\frac{M}{L_s}.\psi_s I_{qr} \quad (14)$$

Assuming that the resistance of the stator winding Rs is neglected, the voltage equations and the flux equations of the stator windings can be simplified in steady state as:

$$\begin{cases} V_{ds} = 0 \\ V_{qs} = \omega_s.\psi_s = V_s \end{cases} \quad (15)$$

$$\begin{cases}\psi_{ds}=\psi_s=L_sI_{ds}+M_{sr}I_{dr}\\ \psi_{qs}=0=L_sI_{qs}+M_{sr}I_{qr}\end{cases} \quad (16)$$

Since the stator voltage frequency is set by the grid, the rotor speed is deduced from:

$$\omega_r=\omega_s\text{-}P\Omega_{mec} \quad (17)$$

The angle θ_r is obtained by integrating the previous equation:

$$\theta_r=\theta_{r0}+\int_0^t \omega_r.dt \quad (18)$$

The stator active and reactive powers and the rotor voltages can be written according to the rotor currents as:

$$\begin{cases}P_s=-V_s\dfrac{M_{sr}}{L_s}I_{qr}\\ Q_s=V_s\dfrac{\psi_s}{L_s}-V_s\dfrac{M_{sr}}{L_s}I_{dr}\end{cases} \quad (19$$

$$\begin{cases}V_{dr}=R_rI_{dr}-s\omega_s\left(L_r-\dfrac{M_{sr}^2}{L_s}\right)I_{qr}\\ V_{qr}=R_rI_{qr}+s\omega_s\left(L_r-\dfrac{M_{sr}^2}{L_s}\right)I_{dr}+s\dfrac{M_{sr}V_s}{L_s}\end{cases} \quad (20)$$

A complete RSC controller is depicted in Fig.4.

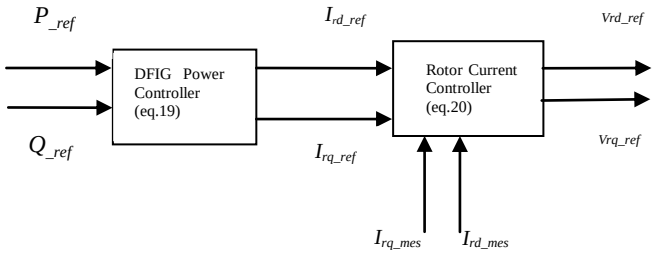

Fig. 4. Rotor side converter control bloc diagram

3.2 Grid side converter control

The grid side converter is charged to regulate the direct current link voltage [17] in manner to fix the reference inverter voltages ($V_{md\text{-}ref}$, $V_{mq\text{-}ref}$) which ensure the control of the delivered current to the grid through the filter. This control is realized by using a reference frame synchronized with the grid voltages. Thus, active and reactive powers transferred to the grid are independently controlled by the delivered currents (I_{td}, I_{tq}) [19]. A complete grid control scheme is depicted in figure 5.

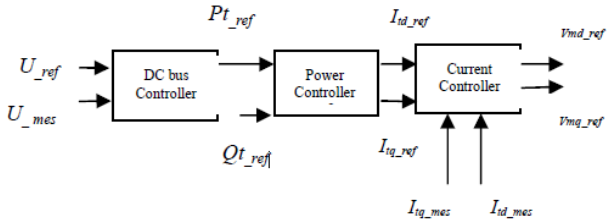

Fig 5. Grid side converter control bloc diagram

By looking this diagram, grid side converter control is based on three functionalities:

DC bus control

The active power reference is derived from the DC bus voltage error (outer PIU controller). This power is obtained after being added to the active power which is necessary to charge the capacitor to the desired value (P_{c_ref}), the DFIG active power generated ($P_{\_mac}=I_{m\text{-}mac}\,U_{\text{-}ref}$) as shown in figure 6.

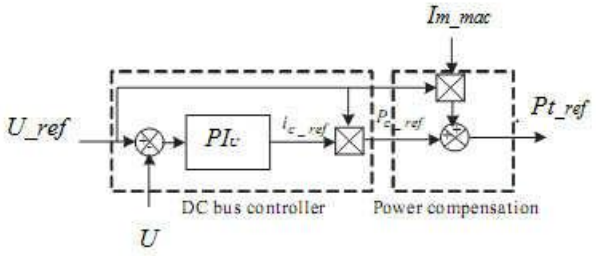

Fig. 6. DC bus control bloc diagram

Power control

The active and reactive powers exchanged with a grid can be expressed by:

$$P_t=v_{sd}i_{td}+v_{sq}i_{tq} \quad (21)$$

$$Q_t=v_{sq}i_{td}-v_{sd}i_{tq} \quad (22)$$

We can find the reference currents i_{td_ref} , i_{tq_ref} , which allows setting the desired reference active and reactive powers P_{t_ref}, Q_{t_ref}, as follows:

$$i_{td-ref} = \frac{P_{t-ref} v_{sd} + Q_{t-ref} v_{sq}}{v_{sd}^2 + v_{sq}^2} \tag{23}$$

$$i_{tq-ref} = \frac{P_{t-ref} v_{sq} - Q_{t-ref} v_{sd}}{v_{sd}^2 + v_{sq}^2} \tag{24}$$

In our case, the reference reactive power is fixed to zero value in order to maintain power factor at unity. We can also generate or absorb the reactive power (Qt_ref <0 or Qt_ref >0).

Current control

Two fast PI current control loops are used to control the grid current vector dq components (i_{td}, i_{tq}) by using the synchronized reference with the grid voltage [11].

The electric equations of the filter (R_t, L_t) connected to the grid are given as:

$$V_{md} = R_t i_{td} + L_t \frac{di_{td}}{dt} - L_t \omega_s i_{tq} + v_{sd} \tag{25}$$

$$V_{mq} = R_t i_{tq} + L_t \frac{di_{tq}}{dt} + L_t \omega_s i_{td} + v_{sq} \tag{26}$$

The grid currents (i_{td}, i_{tq}) can be expressed by the following equations:

$$\frac{di_{td}}{dt} = \frac{1}{L_t}(V_{bd} - R_t i_{td}) \tag{27}$$

$$\frac{di_{tq}}{dt} = \frac{1}{L_t}(V_{bq} - R_t i_{tq}) \tag{28}$$

With:

$$\begin{aligned} V_{bd} &= L_t \omega_s i_{tq} + v_{sd} \\ V_{bq} &= L_t \omega_s i_{td} + v_{sq} \end{aligned} \tag{29}$$

3.3. Storage system control

The third controller is charged to control the energy storage in the flywheel. It is designed to smooth wind power fluctuations by releasing or absorbing stored energy during wind fluctuations. It is well known that the wind speed is fluctuant and, because of this, the wind generator delivers a variable electrical power. To overcome this drawback, an auxiliary energy storage system is installed in order to produce an additional energy and regulate the electric power delivered to the grid [2]. The reference active power applied to the FESS is obtained by:

$$P_{f-ref} = P_{g-ref} - P_{eol} \tag{30}$$

Where Pg_ref the reference grid active power, fixed to -1.5MW value and $Peol$ is the power generated by the DFIG.

3.3.1 Induction machine model

The IM modeled in the Park reference frame [4, 5, 7, 12], is described by:

$$\frac{d}{dt}\begin{pmatrix}\varphi_{rd}\\ \varphi_{rq}\\ i_{sd}\\ i_{sq}\end{pmatrix} = \begin{pmatrix} -\frac{R_{r-IM}}{L_{r-MAS}} & (\omega_s - p\Omega_f) & \frac{M.R_{r-IM}}{L_{r-IM}} & 0 \\ -(\omega_s - p\Omega_f) & -\frac{R_{r-IM}}{L_{r-IM}} & 0 & \frac{M.R_{r-IM}}{L_{r-IM}} \\ \frac{M.R_{r-IM}}{\sigma L_{s-IM} L_{r-IM}^2} & \frac{M.p\Omega_f}{\sigma L_{s-IM} L_{r-IM}} & -\frac{R_{sr}}{\sigma L_{s-IM}} & \omega_s \\ -\frac{M.p\Omega_f}{\sigma L_{s-IM} L_{r-IM}} & \frac{M.R_{r-IM}}{\sigma L_{s-IM} L_{r-IM}^2} & -\omega_s & -\frac{R_{sr}}{\sigma L_{s-IM}} \end{pmatrix} \begin{pmatrix}\varphi_{rd}\\ \varphi_{rq}\\ i_{sd}\\ i_{sq}\end{pmatrix} + \begin{pmatrix} 0 & 0 \\ 0 & 0 \\ \frac{1}{\sigma L_{s-IM}} & 0 \\ 0 & \frac{1}{\sigma L_{s-IM}} \end{pmatrix} \begin{pmatrix} v_{sd} \\ v_{sq} \end{pmatrix} \tag{31}$$

The rotor flux oriented control is applied to the IM, the system (31) becomes:

$$\frac{d}{dt}\begin{pmatrix}\varphi_{rd}\\ i_{sd}\\ i_{sq}\end{pmatrix} = \begin{pmatrix} -\frac{R_{r-IM}}{L_{r-IM}} & \frac{M.R_{r-IM}}{L_{r-IM}} & 0 \\ \frac{M.R_{r-IM}}{\sigma L_{s-IM} L_{r-IM}^2} & -\frac{R_{sr}}{\sigma L_{s-IM}} & \omega \\ -\frac{M.p\Omega_f}{\sigma L_{s-IM} L_{r-IM}} & -\omega & -\frac{R_{sr}}{\sigma L_{s-IM}} \end{pmatrix} \begin{pmatrix}\varphi_{rd}\\ i_{sd}\\ i_{sq}\end{pmatrix} + \begin{pmatrix} 0 & 0 \\ \frac{1}{\sigma L_{s-IM}} & 0 \\ 0 & \frac{1}{\sigma L_{s-IM}} \end{pmatrix} \begin{pmatrix} v_{sd} \\ v_{sq} \end{pmatrix} \tag{32}$$

The rotor-flux reference value can be computed using the flux weakening algorithm. It is determined by [15]:

$$\varphi_{r-ref}(\Omega_f) = \begin{cases} \varphi_{rn} & \text{if} \quad |\Omega_f| \le \Omega_{fn} \\ \varphi_{rn} \cdot \dfrac{\Omega_{fn}}{|\Omega_f|} & \text{if} \quad |\Omega_f| > \Omega_{fn} \end{cases} \tag{33}$$

The reference power of the FESS, Pf_ref, must be limited to the rated value of the IM power in order to avoid the IM overheating. The torque reference is given by:

$$T_{em-IM-ref} = \frac{P_{f-ref}}{\Omega_f} \quad (34)$$

The quadratic reference current becomes:

$$i_{sq-ref} = \frac{T_{em-IM-ref} \cdot L_{r-IM}}{p.M.\varphi_{rd-ref}} \quad (35)$$

A complete flywheel control scheme is depicted in figure 7.

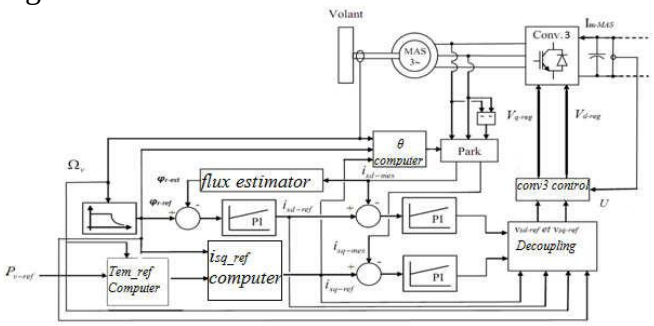

Fig 7. FESS system control scheme.

4. Simulation results

To study the final control solution, both storage controller and the wind power conversion system have been tested and all simulations were carried out using Matlab/Simulink. The DFIG was rated at 1.5MW and its parameters are given in appendix. The DC link voltage was set at 2000V and the capacitance is 4400µF. The results shown here are for the conditions where reactive power *Qg_ref* =0 and active power *Pg_ref* = -1.5MW as shown in figures 10 and 11.

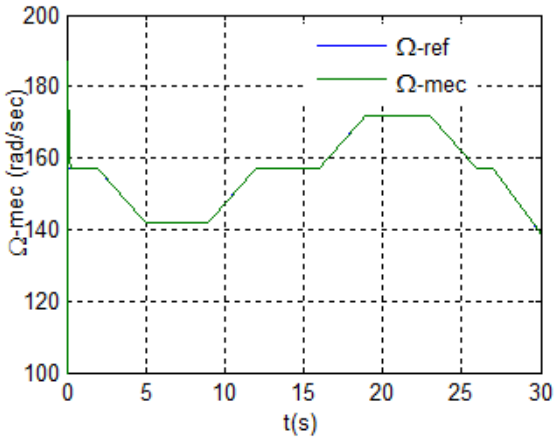

Fig. 8. Random of the DFIG rotor speed

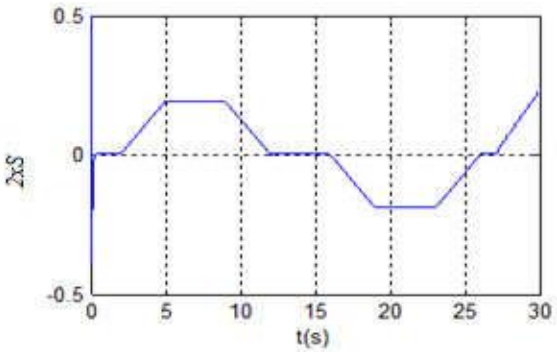

Fig. 9. DFIG slip.

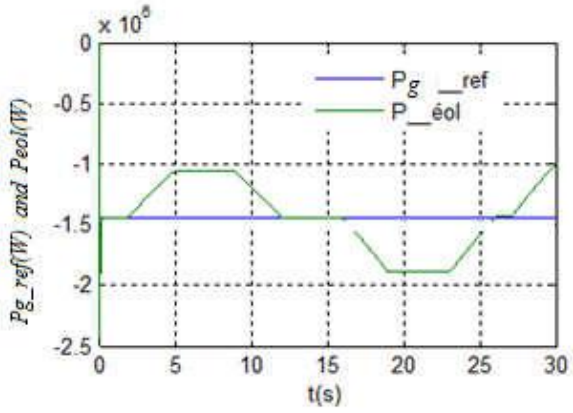

Fig. 10. DFIG active power.

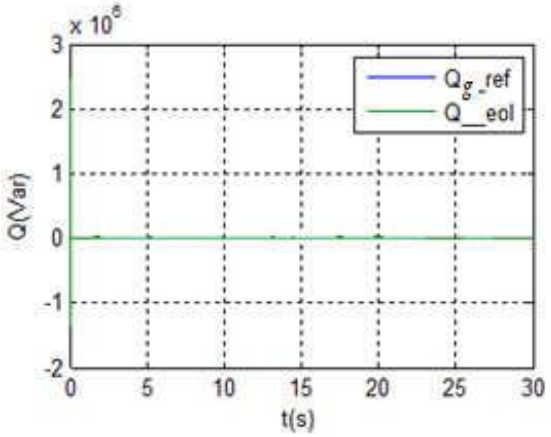

Fig. 11. DFIG reactive power.

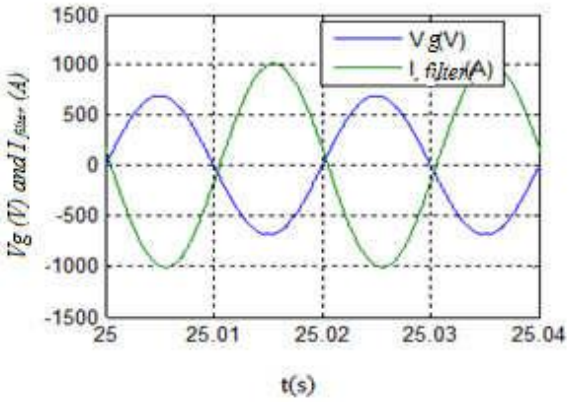

Fig. 12. Grid voltage and current

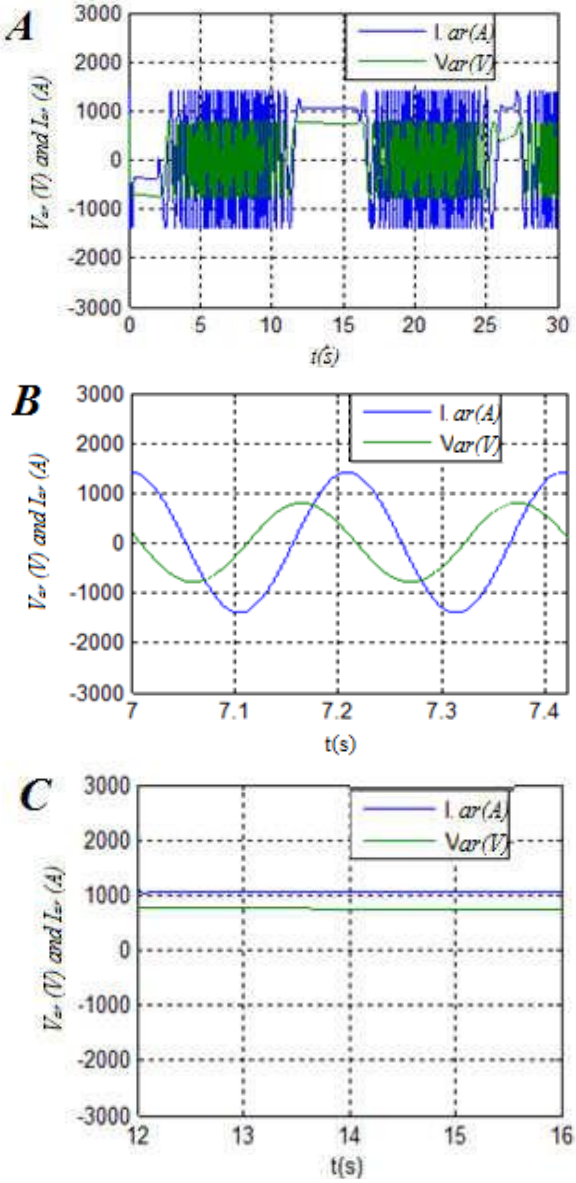

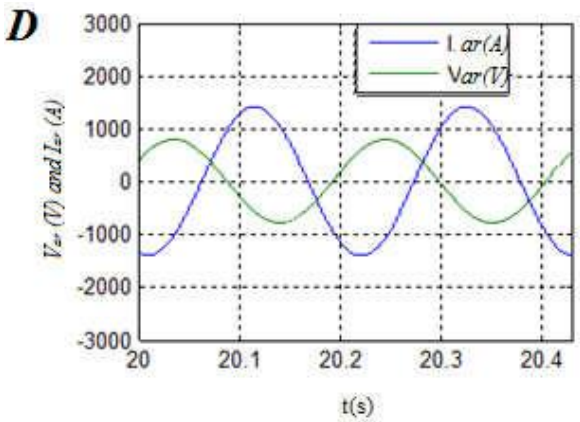

Fig. 13. (A) Rotor current and voltage. (B) zoom of rotor current and voltage for s>0.(C) zoom of rotor current and voltage for s=0. (D) zoom of rotor current and voltage for s<0.

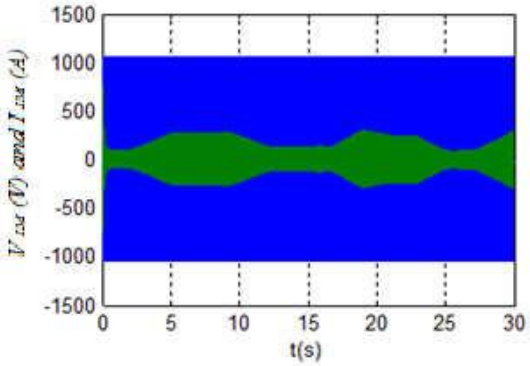

Fig. 14. IM stator voltage and current

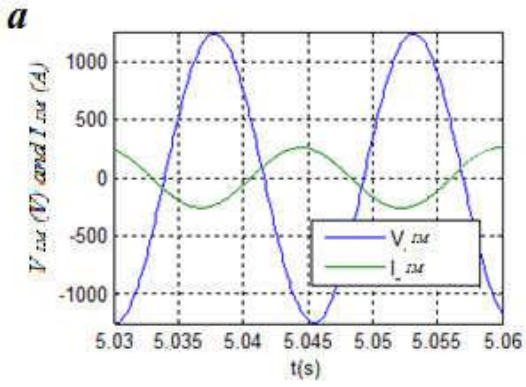

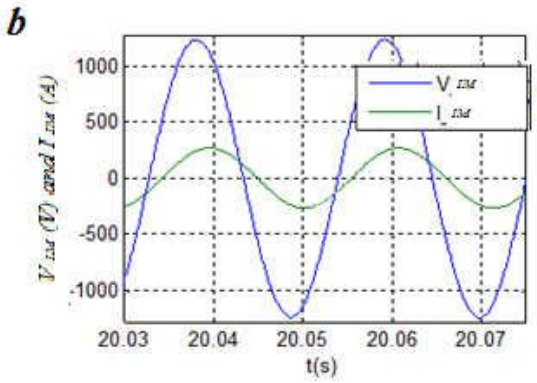

Fig. 15. (a) IM stator voltage and current for s>0
(b) IM stator voltage and current for s<0

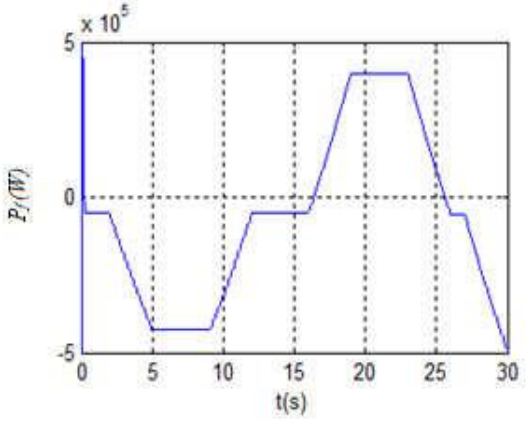

Fig. 16. Delivered FESS power

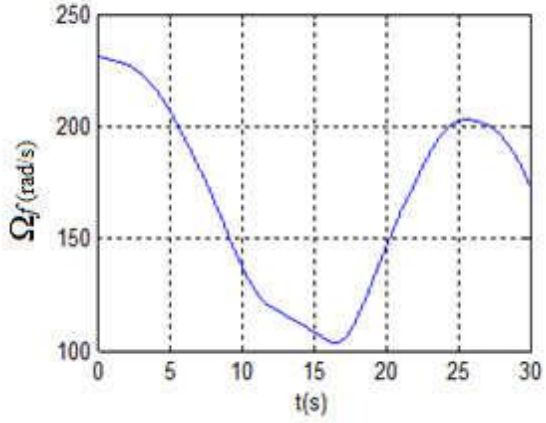

Fig. 17. FESS speed

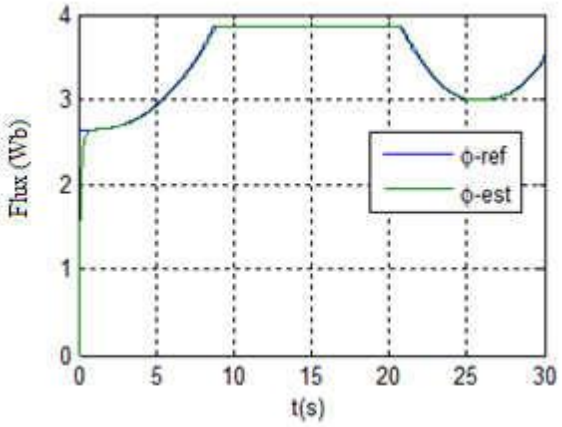

Fig. 18. Direct component IM rotor flux

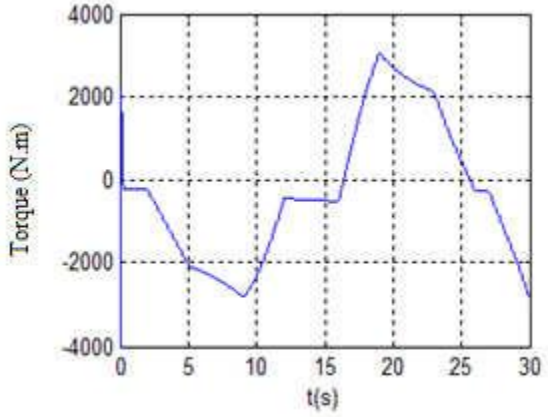

Fig. 19. IM electromagnetic torque

The DFIG rotor speed random and the slip are shown in figures 8 and 9. The grid voltage and current are in phase opposition which implies that the machine supplies the grid only with active power (fig 12). According to the slip, the rotor current and voltage and their zoom are presented in figure 13a-d. When s=0, the rotor absorbs an active power under drop form and the rotor voltage and current are continuous. The stator voltage and current waveforms of the IM are shown, respectively, in Fig.14a–b. The wind power generated variation causes a variation of the active power exchanged between the grid and the FESS which slowdowns/accelerates as shown in figures 16 and 17. Figure 18 shows that the IM stator flux changes as a function of the speed which shows that the IM operates in the flux weakening region. Figure 19 presents the IM electromagnetic torque.

5. Conclusion

In this study, a control of a variable speed wind generator system based on a doubly fed induction generator connected to the network associated to a flywheel energy storage system is considered. Firstly, the doubly fed induction generator is modeled and simulated. A decoupled dq control is adopted for both GSC and RSC. In the second part, the FESS including an IM is proposed and studied. In all DFIG operating mode, the machine supplies the grid only with active power. When s<0, DFIG operates in super-synchronous and the FESS cover the deficit and the IM operates in generator mode. For s>0, DFIG operates in sub-synchronous and the FESS stores the energy surplus and the IM operates in motor mode. When s=0, DFIG operates as synchronized asynchronous generator and the rotor voltage and currents are continuous. The FESS associated to a VSWG is validated by simulation results.

References

[1] Revue Deutscland N° 2, Avril/mai, 2006.

[2] D.Aouzellag, K.Ghedamsi, E.M.Berkouk, Network Power Flow Control of The Wind Generator, Elsevier, Renewable Energy, inpress, 2009.

[3] V. Courtecuisse, Supervision d'une centrale multi sources à base d'éoliennes et de stockage d'énergie connectée au réseau électrique, thèse de doctorat en génie électrique, l'École Nationale Supérieure d'Arts et Métiers, 2008.

[4] A. Davigny, Participation aux services système de fermes d'éoliennes à vitesse variable intégrant du stockage inertial d'énergie, thèse de doctorat en genie électrique, Université des Sciences et Technologies de Lille, 2004.

[5] L.Leclercq, Apport du stockage inertial associé à des éoliennes dans un réseau électrique en vue d'assurer des services systèmes, Thèse de doctorat. Ecole doctorale sciences pour l'ingénieur, Université des Sciences et Technologie de Lille, 2004.

[6] T.Zhou, Commande et Supervision Energétique d'un Générateur Hybride Actif Eolien incluant du Stockage sous forme d'Hydrogène et des Super- Condensateurs pour l'Intégration dans le Système Electrique d'un Micro Réseau, thèse de doctorat en Génie électrique, Ecole Centale de Lille,2009.

[7] G.Cimuca, Système inertiel de stockage d'énergie associé a des générateurs éoliens, Thèse de doctorat, université de Lille, 2004.

[8] G.Esmaili, Application of Advanced Power Electronics in Renewable Energy Sources and Hybrid Generating Systems, Degree Doctor of Philosophy thesis, Ohio State University, 2006.

[9] L.Khetteche, Etude et Commande d'un Système Eolien à Base d'une Machine Electrique Double Alimentée, thèse de Magister en électrotechnique, université de Batna, 2007.

[10]H. E. M.LOPEZ, Maximum Power Tracking Control Scheme for Wind Generator Systems, Master of Science in Electrical Engineering, Texas A&M University, 2007.

[11]S.EL-Aimani, B, Françoi, F. Minne, B.Robyns, "Modeling and simulation of doubly fed induction generators for variable speed wind turbines integrated in a distribution network" 10th European conference on power electronics and applications, (EPE), Toulouse, France, 2-4 September 2003.

[12]L.Baghli, Contribution à la commande de la machine asynchrone, utilisation de la logique floue, des réseaux de neurones, et des algorithmes génétiques, thèse de doctorat en génie électrique, université Henri Poincaré, Nancy-I, 1999.

[13]B. Multon, X.Roboam, B.Dakyo, C.Nichita, O.Gergaud, H.Ben Ahmed, Aérogénérateurs électriques, Techniques de l'ingénieur, D3960, 2004.

[14]S. EL Aimani, modélisation des différentes technologies d'éoliennes intégrées dans un réseau de moyenne tension, thèse de doctorat 2005.

[15]M.Chebre, M.Zerikat, Y.BENDAHA, Adaptation des Paramètres d'un Contrôleur PI par un FLC Appliqué à un Moteur Asynchrone, 4th International Conference on Computer Integrated Manufacturing CIP'2007.

[16]A. Boyette, Contrôle-Commande d'un Générateur Asynchrone à Double Alimentation avec Système de Stockage pour la Production Eolienne, Thèse de Doctorat De l'Université Henri Poincaré, Nancy I, Décembre 2006.

[17]Nicholas P. W. Strachan, J.Dragan, Improving Wind Power Quality using an Integrated Wind Energy Conversion and Storage System (WECSS), IEEE 2009.

[18]T.Ghennam, E.M.Berkouk, B.Francois, Modeling and Control of a Doubly Fed Induction Generator (DFIG) Based Wind Conversion System, IEEE transaction, 2009.

Appendix

Parameters

Blades number: 3, R=35.25 m, G=90,

J (Turbine+DFIG) = 1000 kg/m^2, ρ =1.22 Kg/m^3, P_{DFIG}=1.5MW, R_s =0.012Ω, R_r =0.021Ω, M_{sr} =0.035 H,

L_s =0.035+2.037.10^{-4} H, L_r =0.035+1.75.10^{-4} H, P=2,

f=0.0024 N.m.s/rd, V_s=690V.

IM and FESS parameters: v_s=690V, P_f =450kW,

R_{s-IM} =0.051 Ω, R_{r-IM} =0.051 Ω,

L_{s-IM} = 40.71.10^{-3} H, L_{r-IM} =40.71.10^{-3} H, M =40.1.10^{-3}H, p=2,

f_v=0.008 N.m.s/rd, J_v =250 kg/m^2

Nomenclature

Turbine

$\Omega_{turbine}$: Turbine speed

Ω_{mec} : Generator chaft speed

υ : Wind velocity

R: Rotor radius.

ρ: Air density

S: Area swept by the blades.

C_g: Driven torque of the generator,

G: Gear ratio.

DFIG

V_{ds}, V_{qs}, V_{dr}, V_{qr}: Two-phase stator and rotor voltages

Ψ_{ds}, Ψ_{qs}, Ψ_{dr}, Ψ_{qr}: Two-phase stator and rotor fluxes

R_s, R_r: Stator and rotor phase resistances

L_s, L_r: Stator and rotor phase inductances

I_{ds}, I_{qs}, I_{dr}, I_{qr} : Two-phasestator and rotor currents

s: Generator slip

P: Number of pole pairs

f: Viscous friction

IM and flywheel

v_{sd}, v_{sq}: Two-phase stator voltages

φ_{rd}, φ_{rq}: Two-phase rotor fluxes

$R_{s\text{-}IM}$, $R_{r\text{-}IM}$: Stator and rotor phase resistances

$L_{s\text{-}IM}$, $L_{r\text{-}IM}$: Stator and rotor phase inductances

I_{sd}, i_{sq}: Two-phasestator and rotor currents

σ: Dispersion ratio

p: Number of pole pairs

Ω_f: FESS angular speed

φ_{rn}: Nominal rotor flux

Ω_{fn}: Nominal FESS speed

P_f: FESS active power

$T_{em\text{-}IM}$: FESS electromagnetic torque